Micro-scale viscosity measurements of different thermotropic and lyotropic classes of liquid crystals by using ferrofluid inclusions

DOI:
10.1016/j.molliq.2023.122178

Document Version
Final published version

Journal of Molecular Liquids 383 (2023) 122178

Contents lists available at ScienceDirect

Journal of Molecular Liquids

journal homepage: www.elsevier.com/locate/molliq

Micro-scale viscosity measurements of different thermotropic and lyotropic classes of liquid crystals by using ferrofluid inclusions

Varun Chandrasekar, Jian Ren Lu, Ingo Dierking *

Department of Physics and Astronomy, University of Manchester, Oxford Road, Manchester M139PL, UK

ARTICLE INFO

Keywords:
Liquid crystal
Viscosity
Nematic
Smectic
Thermotropic
Lyotropic
Chromonic
Colloidal liquid crystal

ABSTRACT

Dispersing micro- and nanoparticles in liquid crystals (LCs) is utilised to tune liquid crystal properties, to add functionality or to exploit the self-organization of the liquid crystals to transfer order onto dispersed particles. Dispersing ferrofluid droplets in LCs produces a system similar to LC-microparticle dispersions, because the ferrofluid droplets behave in first approximation as non-compressible, only slightly deformable particles. Such a LC-ferrofluid system adds a magnetic functionality, which can be exploited to measure the viscosity and its anisotropy on a microscopic scale when moving the ferrofluid inclusions through various liquid crystals of the thermotropic, lyotropic or colloidal kind. Effective viscosities can be determined as a function of changing environment, such as temperature or concentration, and for variation of other factors such as the pitch of chiral phases for instance. The viscosities are calculated using Stokes' Law together with the introduction of a boundary layer at the liquid crystal – ferrofluid interface. We present results for a variety of different liquid crystalline systems; thermotropic nematics, chiral nematics, smectics, lyotropic phases and chromonic systems, as well as colloidal LCs such as cellulose nanocrystals (CNC) and graphene oxide (GO) varying the viscosity over more than three orders of magnitude. The results are discussed in terms of the structures of respective phases.

1. Introduction

Liquid crystals (LCs) [1,2] often referred to as mesophases, are partially ordered, anisotropic, self-organized phases, which are thermodynamically located between the three-dimensional crystalline solid and the isotropic liquid [3]. LCs exhibit the fluid properties of conventional liquids and at the same time show the anisotropic properties of crystalline solids. Although there are various ways of classifying LCs depending on molecular features and supramolecular assemblies; the most commonly used classification is based on how the LC phases have been obtained, namely thermotropic through temperature changes and lyotropic through concentration changes of a dispersant in an isotropic solvent [4].

Thermotropic LCs [2,5] are distinguished by their degree of order, showing further phase transitions within the temperature regime of the liquid crystalline state [6]. The different phases exhibited in our study are isotropic, nematic, cholesteric (also referred to as chiral nematic phase) and smectic A. Lyotropic LCs [5,7,8] are observed when changing the concentration of a dispersant, such as amphiphilic molecules, in an isotropic solvent, often water [9]. At concentrations above the critical micelle concentration (cmc), the molecules form micellar aggregates which are randomly distributed in the solvent. At even higher concentrations, these micelles can aggregate to form LC phases. The phase transitions between the LC phases depend largely on the concentration of the dispersant and on the temperature [10].

Some of the most detailed and precise viscosity measurements of LCs were performed by Kneppe and Schneider [11,12]. Their apparatus consisted of a capillary connected at each end to a closed vessel filled with nitrogen and a change of the pressure in one vessel induces a flow of the liquid crystal through the capillary. By measuring the pressure difference between the vessels as function of time the viscosity coefficients of the thermotropic LC MBBA (4-methoxy-benzylidene-4′-n-butylaniline) were determined [12]. Another example of earlier viscosity measurements is the work by Chmielewski [13]. The measurement method involved the use of a slot viscosimeter and an electromagnet to measure the viscosities of the standard cyano-biphenyl LCs 5CB, 8CB, 5OCB and 8OCB. In terms of lyotropic LCs, viscosity measurements are less common than those for thermotropic liquid crystals. In the work by Liu et al., [14] the viscosities of the cholesteric and lamellar phases of the sodium decyl sulfate-decanol-water (SDS/1-

* Corresponding author.
E-mail address: ingo.dierking@manchester.ac.uk (I. Dierking).

https://doi.org/10.1016/j.molliq.2023.122178
Received 19 March 2023; Received in revised form 3 May 2023; Accepted 21 May 2023
Available online 25 May 2023

decanol/water) ternary system were measured using laser tweezers and rotating laser-trapped optically anisotropic microspheres. For graphene oxide (GO), Ansón-Casaos et al., [15] used Ubbelohde capillary viscosimeters to measure the effect of nanoparticle shape, concentration, degrees of motion and surface chemistry on the viscosity of dilute dispersions of GO.

In a classic paper by Poulin et al., [16] LC-water emulsions were created by dispersing water droplets in 5CB with the help of the surfactant sodium dodecyl sulphate. Here, chains of water droplets were obtained in the LC and the droplets were held together by dipolar defects in the LC. Poulin et al., [17] also employed ferrofluid droplets as a means to measure the attractive interactions between colloidal particles suspended in a nematic LC. One example of dispersing ferrofluids in lyotropic nematic LCs (not for viscosity measurement though) is the work done by Neto and Saba, in which they observed a mixture of potassium laurate (28.74 wt%)/Decanol (6.64 wt%)/H_2O (64.62 wt%) doped with different concentrations of ferrofluids under a polarizing microscope to determine the minimum concentration of ferrofluid above which the liquid-crystalline matrix is oriented by the ferrofluid grains [18]. In this study we employ micrometre-sized ferrofluid droplets to determine the viscosities of both thermotropic and lyotropic liquid crystalline systems. The method has the advantage that it can be applied to very small sample volumes and does not need much material. At the same time, values are obtained which are very similar to those measured by methods using sample volumes which are orders of magnitude larger [11–13].

Our investigation here is an extension based on our previous work [3]. When a ferrofluid is dispersed in a liquid crystal, micrometer sized droplets with different diameters are formed which can be moved using a permanent magnetic field. With this method we are measuring the kinematic viscosities of LCs on a microscopic scale by using Stokes' law for a sphere moving through the LC. For these measurements the magnetic Fredericks transition [19] needs to be avoided, because this would cause the director of the LC to reorient and effectively result in measuring the incorrect anisotropic viscosity. Therefore, the magnetic field employed needs to be below the magnetic threshold Fredericks field.

2. Materials and methods

The thermotropic liquid crystals studied include 5CB (4-Cyano-4′-pentylbiphenyl), 8CB (4-cyano-4′-octylbiphenyl) and 5CB + chiral dopant S811 (S-(+)-2-Octyl 4-(4-hexyloxybenzoyloxy) benzoate). The lyotropic liquid crystals investigated include Sunset Yellow (disodium,6-oxo-5-[(4-sulfonatophenyl) hydrazinylidene] naphthalene-2-sulfonate) as a chromonic lyotropic and CTAB (Hexadecyl trimethyl ammonium bromide) as an amphiphilic lyotropic. The colloidal liquid crystals studied are graphene oxide (GO) and cellulose nanocrystals (CNCs), both in deionized water. 5CB and 8CB were purchased from Fluorochem and the chiral dopant S811 was obtained from Xian Hua, China. The chromonic dye Sunset Yellow was purchased from Instant-Sunshine, and CTAB from Sigma-Aldrich. CNCs were purchased from Nanografi Nano Technology and GO flakes were purchased from William Blythe Ltd. The respective chemical structures are shown in Fig. 1. The ferrofluids used are the water based WHKS1S12, which was obtained from Liquid Research Ltd, UK, for the investigations on the thermotropic LCs, and the oil based EFH1 which was purchased from Ferrotech, USA for studying lyotropic LCs. The reason for using different ferrofluids is that a phase separated emulsion is required and the carrier fluid of the ferrofluid should not mix with the LC. All materials were used as purchased.

The motion of the spherical ferrofluid droplets in the LCs and their positions are imaged using either a Leica or a Nikon polarized optical microscope (POM). Self-constructed sandwich cells of thickness 75–120 μm are filled with the LC-ferrofluid emulsion and placed under the objective of the POM. The motion of the ferrofluid droplets is recorded using an IDS camera (uEye COCKPIT) (Fig. 2(a)) and the positions are measured using the Trackmate plugin in Fiji (ImageJ). From the linear dependence of position as a function of time, the droplet velocity is determined (Fig. 2(b)).

The methodology is illustrated in more detail in Fig. 3. Starting at an arbitrary time t = 0 s with the magnetic field applied, the ferrofluid droplet moves through the liquid crystal at constant speed, the displacement being $h_{perp}(t)$ and $h_{para}(t)$, with the directions referring to perpendicular and parallel direction to the rubbing direction, i.e. perpendicular and parallel to the substrate edges. The displacements, h (t), are a linear function of time, easily allowing the determination of the velocities perpendicular and parallel to the rubbing direction, which is also perpendicular and parallel to the long molecular axis in the case of a nematic or a smectic A phase. Fig. 3(a) and (b) show a time series of this motion for illustration, with the determined data depicted in Fig. 3(c).

3. Experiments

To create the LC-ferrofluid emulsion, the ferrofluids WHKS1S12 and EFH1 are mixed with thermotropic LCs and lyotropic LCs respectively. For WHKS1S12, the ferrofluid is sonicated to remove any aggregates. The ferrofluid is selected to ensure that the carrier fluids do not mix with the surrounding LC, which would otherwise lead to dissolution of the carrier fluid and aggregation of the ferrofluid's magnetite particles. For each emulsion, the ferrofluid is added to the LC in the ratio of ≈ 2:100 and the mixture is vortexed using an IKA Vortex Genius 3 mixer to obtain a homogeneous emulsion. A glass sandwich cell is then prepared with each glass plate being coated with PVA and unidirectionally rubbed after baking for 20 mins to obtain planar anchoring boundary conditions. The LC-ferrofluid emulsion is filled into the sandwich cell and the edges of the cell are sealed using an Epoxy glue. The LC is oriented in the sandwich cell by the PVA coated on the glass plates of the cell and this procedure is done for the different thermotropic and lyotropic LCs studied.

To prepare the thermotropic chiral nematic samples with different pitches, 5CB was doped with the chiral dopant S811 in isopropanol. After sonicating for 1 h and evaporating the solvent for 12 h, the pitch of each chiral nematic was measured using the fingerprint method. Then, the ferrofluid WHKS1S12 was dispersed to create the LC-ferrofluid emulsions. The LC-ferrofluid emulsions were then filled into the glass sandwich cells by capillary action and both parallel and perpendicular viscosities were measured. The parallel and perpendicular directions are with respect to the direction in which the PVA coated on the glass plates was rubbed.

Following the methodology outlined in reference [3] and the description of ferrofluid magnetisation by Li et al., [20] along with the usage of Stokes' law, the viscosity γ of the liquid crystal is inversely proportional to the equilibrium velocity v_{eq} of the ferrofluid droplet and varies as

$$\gamma = \frac{2r^2 M_{vol}.\nabla \mathbf{B}}{9v_{eq}} \quad (1)$$

when the droplet is dragged through the liquid crystal by a magnetic field. The magnetic colloidal particles in the ferrofluid accumulate at the interface between the ferrofluid and the LC and arrange in such a way that the boundary layer has a net contribution of zero to the magnetization of the ferrofluid droplet (the net magnetization comes from the bulk of the ferrofluid droplet). The boundary layer is independent of the anchoring conditions and droplet size but does depend on the nature of the dispersion [3]. Here, $r = r_m$-b is the effective radius of the droplet (the radius of the measured droplet r_m minus the boundary layer thickness b), ρ is the density of the ferrofluid, μ_0 is the permeability of vacuum and $\mathbf{M_m}$ is the mass magnetization of the ferrofluid from which the volume magnetization $M_{vol} = M_m\rho$ is calculated. ∇H is the gradient of the applied magnetic field intensity with $\nabla B \approx \mu_0 \nabla H$. The values of M_{vol} are 9450 A m^{-1} for WHKS1S12 and 25,300 A m^{-1} for EFH1, as

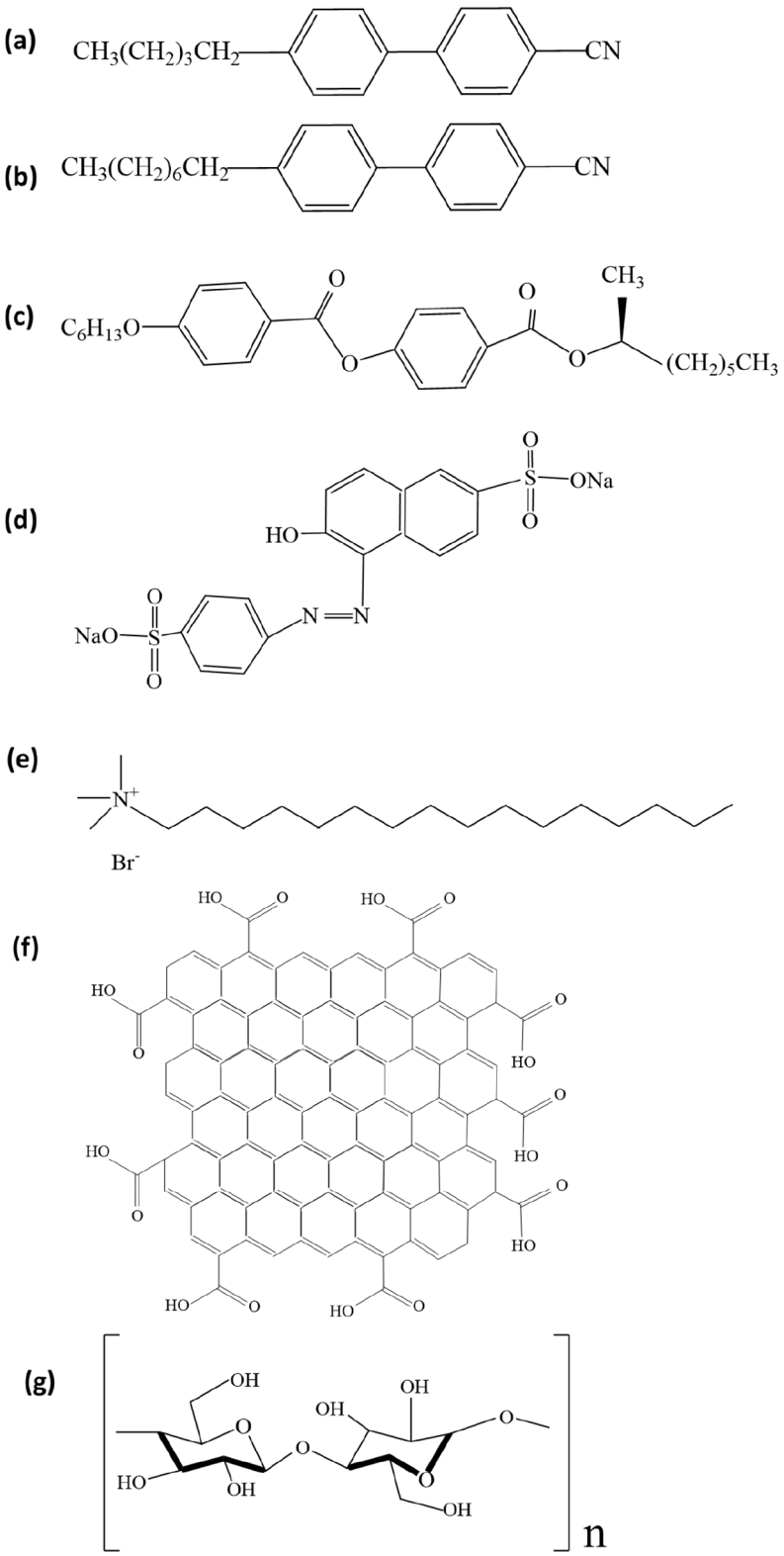

Fig. 1. Chemical structures of the materials investigated: (a) thermotropic nematic 5CB (b) thermotropic nematic and smectic 8CB (c) chiral dopant S811 (d) chromonic dye Sunset Yellow, (e) amphiphilic CTAB and schematics of (f) Graphene Oxide and (g) cellulose.

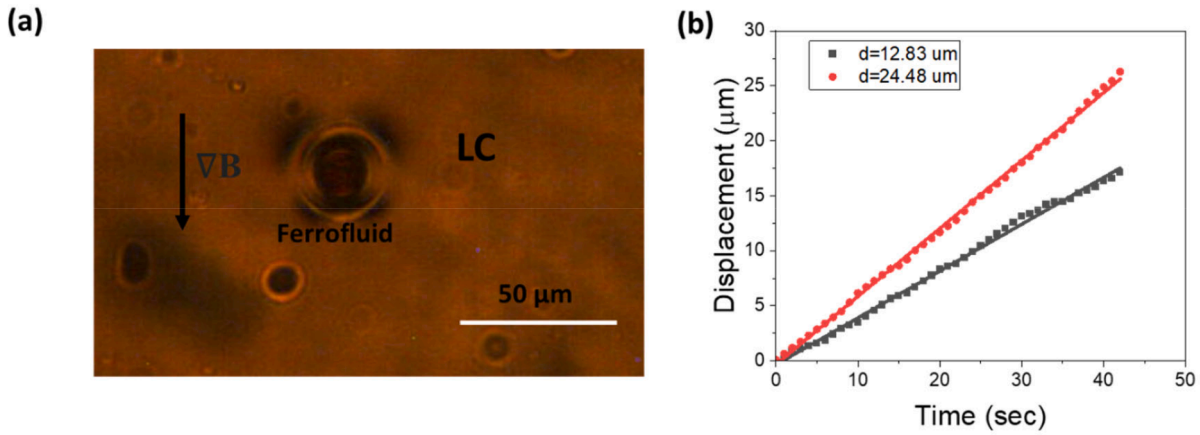

Fig. 2. (a) A micro-droplet of ferrofluid WHKS1S12 in 5CB in a magnetic field gradient, ∇B which is applied parallel to the alignment direction. (b) Displacement vs time in direction parallel to the director of nematic 5CB for two droplets of different diameters d. The relationship is linear, so that the equilibrium velocity, v_{eq}, is given by the slope.

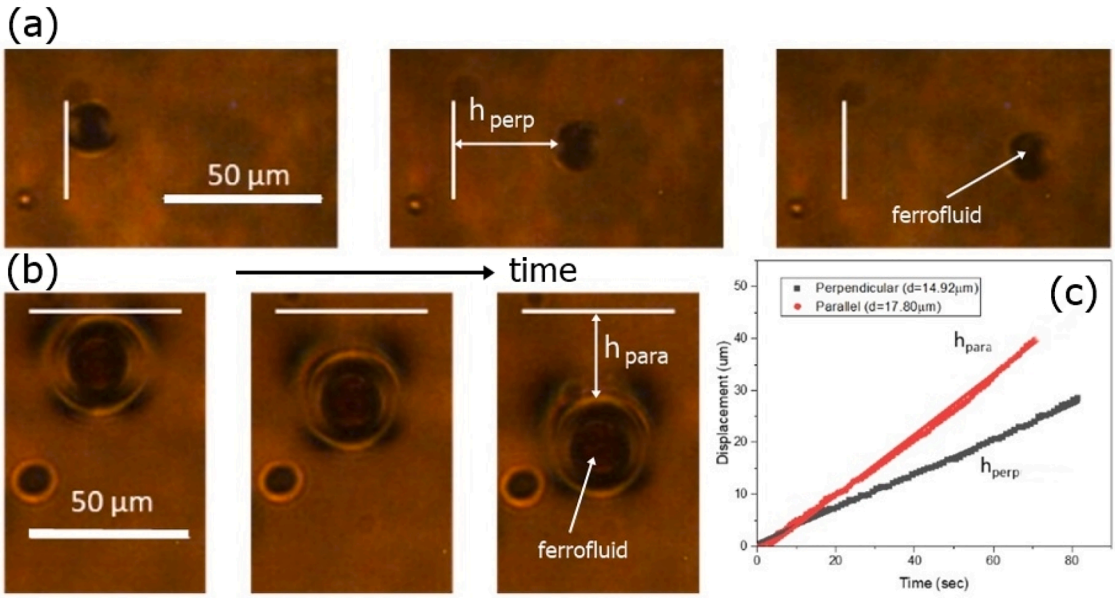

Fig. 3. (a) A micro-droplet of ferrofluid WHKS1S12 moving in 5CB in the perpendicular direction (b) A micro-droplet of ferrofluid WHKS1S12 moving in 5CB in the parallel direction (c) Displacement vs time plot for (a) and (b).

obtained from the respective suppliers. The ferrofluid droplets are not in contact with the glass plates which can be confirmed qualitatively by moving the focal plane. An explanation why particles, and thus also droplets as fluid particles, stay in the middle plane between the bounding substrates was provided by Lavrentovich [21]. It was shown that these are held in the bulk not only by thermal motion, but also by elastic repulsion from bounding glass plates. The droplets are repelled from the glass as the uniform director field near the glass is incompatible with the director distortions around the droplet [21].

To estimate the boundary layer thickness of each ferrofluid-LC combination, the velocities of different droplets of varying sizes are measured. The ratio of the equilibrium velocities v_1 and v_2 of two ferrofluid droplets of different sizes r_1 and r_2 allows the estimation of the boundary layer thickness b:

$$\frac{(r_1 - b)^2}{(r_2 - b)^2} = \frac{v_1}{v_2} \tag{2}$$

4. Results and discussion

4.1. Thermotropic nematic 5CB

The perpendicular and parallel viscosities of 5CB, with respect to the director, were measured and verified against reported values [3,13] for an initial validation. The parallel and perpendicular viscosity values at room temperature (≈21∘C) are $\gamma_{\parallel} = 45 \pm 1$ mPa s and $\gamma_{\perp} = 129 \pm 4$ mPa s, respectively. These values agree well with the values reported by Chmielewski ($\gamma_{\parallel} = 44$ mPa s and $\gamma_{\perp} = 120$ mPa s) [13]. The average boundary layer thickness for WHKS1S12 in 5CB was determined to be 5 ± 1 µm, which is similar to the value reported previously [3] (4.4 ± 0.2 µm). From this, it can be concluded that the employed methodology is reproducible and can thus be applied to other LC systems as well.

4.2. Thermotropic nematic-smectic a transition of 8CB

The viscosities of liquid crystal 8CB (4-cyano-4′-octylbiphenyl) were measured, using the WHKS1S12 ferrofluid in the temperature range

34∘C-39∘C, across the nematic to smectic A phase transition at T_C = 36 °C. To measure the viscosities, the ferrofluid was dispersed in smectic 8CB at room temperature and the emulsion was then heated to 40∘C and filled into a sandwich cell. After placing the system in the POM, the viscosities were measured while increasing/decreasing the temperature using a hot stage of relative accuracy of 0.1 K.

The temperature at which all smectic A islands disappear is observed to be at 36∘C. At this temperature, the measured parallel and perpendicular viscosities are approximately 45 ± 2 mPa s and 130 ± 2 mPa s, respectively (Fig. 4(a)). At higher temperatures, the LC is in the nematic phase. Using the measured velocities and observing the behaviour of ferrofluid droplets with different diameters, the thickness of the boundary layer was also determined for 8CB (see Fig. 4(b)).

The viscosities shown in Fig. 4(a), are in good agreement with the reported values by Chmielewski [13]. It is interesting to notice that the viscosities do not exhibit any discontinuities at the nematic to smectic A transition. The viscosity parallel to the director does not appear to change significantly at all, while the perpendicular viscosity increases continuously as the temperature is lowered. The formation of smectic layers does not have any significant influence on the viscous properties of the LC in the vicinity of the transition. A similar behaviour is observed for the thickness of the boundary layer, which is independent of the drag direction of the ferrofluid droplets within limits of error. Also, the nematic to smectic A phase transition does not have any clear impact on the boundary layer thickness. In the small temperature regime investigated, the latter can thus be averaged to yield a value of approximately 5.3 ± 0.8 μm. We note that this is practically equivalent to the value determined for 5CB, which was to be expected, as the molecular structures of 5CB and 8CB only differ slightly in the length of the flexible chain.

4.3. Thermotropic cholesteric 5CB + S811

The cholesteric or chiral nematic LC phase exhibits a self-organized helical superstructure with the director spiraling as one proceeds in the direction perpendicular to the long molecular axes. [22]. The helical superstructure is characterized by its pitch p and the helix handedness, where p is the distance along which the helix completes a full turn of 360°. The helix handedness changes when the molecular chirality of the mesogen or the chiral dopant is reversed. For chiral nematics, obtained by adding a chiral dopant to an achiral nematic matrix, the pitch p varies as $p = M_{tot}/HTP.m$, where HTP is the helical twisting power, m is the mass of the chiral dopant added and M_{tot} is the total mass. This relation is valid for small dopant concentrations and in the case of dopant S811 in liquid crystal 5CB the HTP was found to be HTP ≈ 8.2 μm^{-1}.

For long pitch samples, the director configuration is strongly influenced by the cell gap, which was chosen here as d = 100 μm. If the pitch is clearly shorter than the cell gap, p ≪ d, a full helical structure with a large number of 2π-twists can develop, for which one would not expect any anisotropy in the plane of the substrate, because all director orientations would be present. As the dopant concentration decreases, the pitch of the helix would increase, such that the confining boundary conditions would distort the helical superstructure, exhibiting an increasing anisotropy with increasing pitch p. Once the dopant concentration is so small that the induced pitch is comparable or larger than twice the cell gap, p ≈ 2d, the helical structure will be unwound by the boundary conditions of the confinement, and one would obtain a nematic director configuration with roughly the same anisotropy as the undoped 5CB.

This is indeed observed for the viscosities of S811 doped 5CB, as depicted in Fig. 5(a). For a structure with the pitch much smaller than the cell gap, the viscosity measurements in two mutually orthogonal directions with respect to the rubbing direction of the PVA on the glass plates of cells yield the same values for the parallel and the perpendicular direction due to the many 2π twists between the two glass plates. This indicates a fully developed helical superstructure with several 2π-twists covering the diameter of the ferrofluid droplet. The fact that the observed value does not lie in the middle between the perpendicular and parallel viscosities of pure 5CB can be attributed to the influence of the chiral dopant which has to be added at its greatest concentration in this pitch regime. In any case, the viscosity value measured perpendicular to the rubbing direction is smaller than that measured for undoped 5CB in the nematic state. At an infinite pitch, i.e., the unwound chiral nematic structure, the previously measured values of 5CB (45 ± 1 mPa s and 129 ± 4 mPa s) are regained.

At a pitch value of p = 20 μm, corresponding to the average diameter of ferrofluid droplet, the parallel and perpendicular viscosities are 86 ± 6 mPa s and 117 ± 5 mPa s, respectively. This indicates that the helical director structure is already considerably distorted, reflected by the anisotropy of the viscosities. From this, one can conclude that the ratios between pitch and cell gap, as well as pitch and ferrofluid droplet diameter are important factors in the determination of the viscosities of helical phases. On the other hand, this also opens the possibility to probe director field variations if the droplet diameter can be suitably controlled, for example, via microfluidics. The boundary layer values for the WHKS1S12 droplets in the chiral nematic samples are shown in

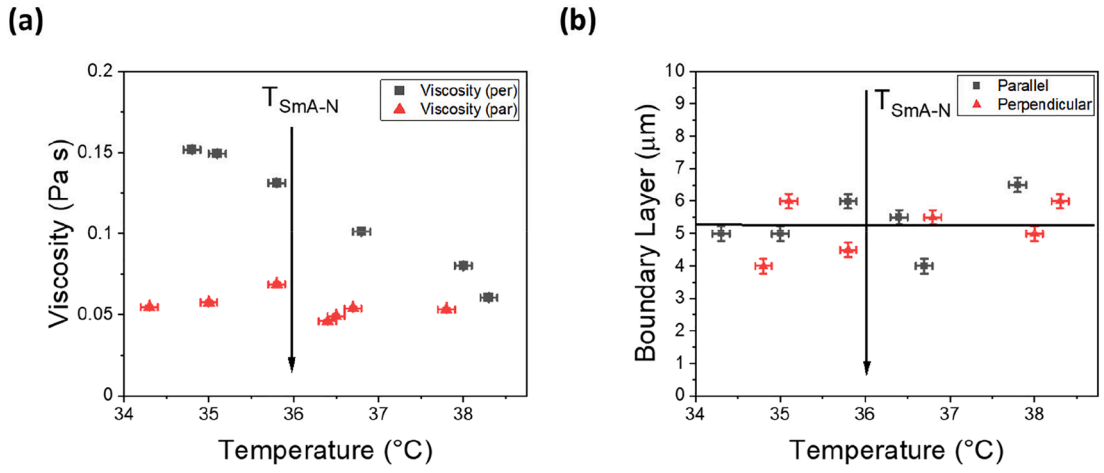

Fig. 4. (a) Measured temperature dependence of the viscosities of 8CB across the nematic to smectic A phase transition. Note that no discontinuous behaviour is observed at the transition and the viscosities change smoothly, with the one parallel to the director being uninfluenced. (b) A similar behaviour is observed for the boundary layer thickness which does not change across the transition.

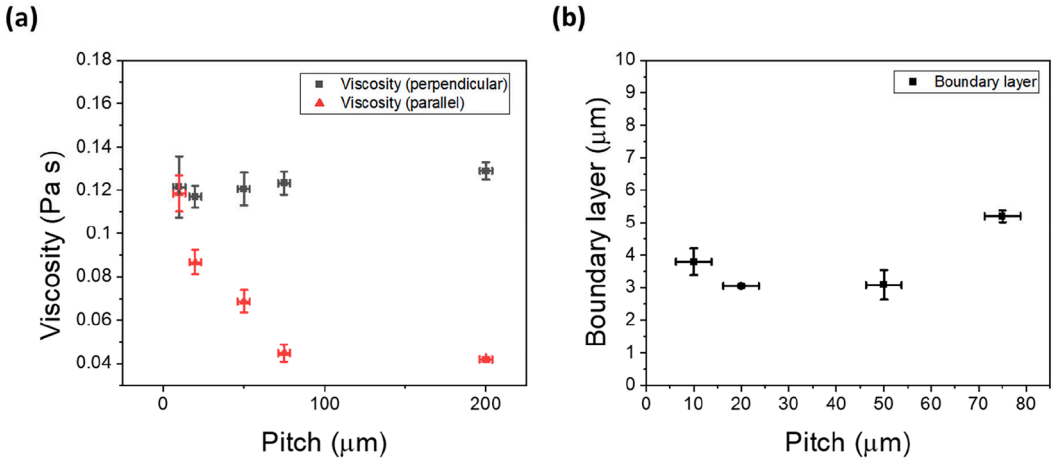

Fig. 5. (a) Viscosity vs pitch for 5CB + S811. For pitch < 20 μm, the average diameter of the ferrofluid droplets, the LC behaves as expected for a chiral nematic, with no anisotropy of viscosity in the substrate plane. As the pitch increases and the helical structure is unwound by the confinement and boundary conditions, the anisotropic values of the nematic phase are regained. (b) The boundary layer is largely independent of the pitch for 5CB + S811, similar to the value of the pure nematic host.

Fig. 5(b) and do not appear to vary much with increasing pitch. They are also similar in magnitude to the boundary layer value of pure 5CB and show an average value of approximate 3.8 ± 1 μm, somewhat lower than the neat nematic, which is most likely due to the addition of the chiral dopant.

4.4. Lyotropic CTAB

Cetyltrimethylammonium bromide (CTAB) is a cationic amphiphile which, when dissolved in water, can exhibit liquid crystalline phases [23,24]. CTAB is one of the standard amphiphilic lyotropic LCs [25]. The anisotropic viscosities of aqueous CTAB solutions in the hexagonal phase and the isotropic phase are measured using the oil-based ferrofluid EFH1. At room temperature, CTAB exhibits a hexagonal LC phase between 20% and 70% concentration. Below 20% concentration, CTAB is in the isotropic phase. The LC phases are oriented using PVA coated glass plates and some of the LC phases such as the hexagonal phase are indeed very difficult to orient in the sandwich cell. In this case the oriented regions are relatively small and the determination of the velocities becomes less accurate. This is reflected in the increasing errors on the determination of the viscosities in the hexagonal phase as compared to the region of the phase diagram where micelle formation is taking place, which results in an isotropic phase and a two-phase region at higher concentrations.

At the cmc (0.05%) [26], the parallel and perpendicular viscosity values are obviously equal in magnitude ($\gamma_{\perp} = 230 \pm 7$ mPa s; $\gamma_{\parallel} = 228 \pm 7$ mPa s). Although the viscosity is isotropic, it is still much larger than the viscosity of water ($\gamma_{water} = 0.89$ mPa s [3]), suggesting that the formation of micelles strongly increases the viscosity (Fig. 6(a)). The boundary layer at very small concentrations just at the cmc is comparable to that of the solvent, water (~2.8 μm), which shows that the aggregation to micelles has proceeded, but that these are quite dispersed within the solvent. The value observed is comparable to that of a standard thermotropic nematic liquid crystal or a viscous isotropic fluid like silicone oil. In the lyotropic hexagonal phase, which is starting at a concentration of approximately 25 wt%, the viscosity becomes anisotropic and the difference between the parallel and perpendicular viscosity values increases with increasing concentration as depicted in Fig. 6(a). The boundary layer thickness also appears to increase with increasing concentration due to the lyotropic phase structure of the

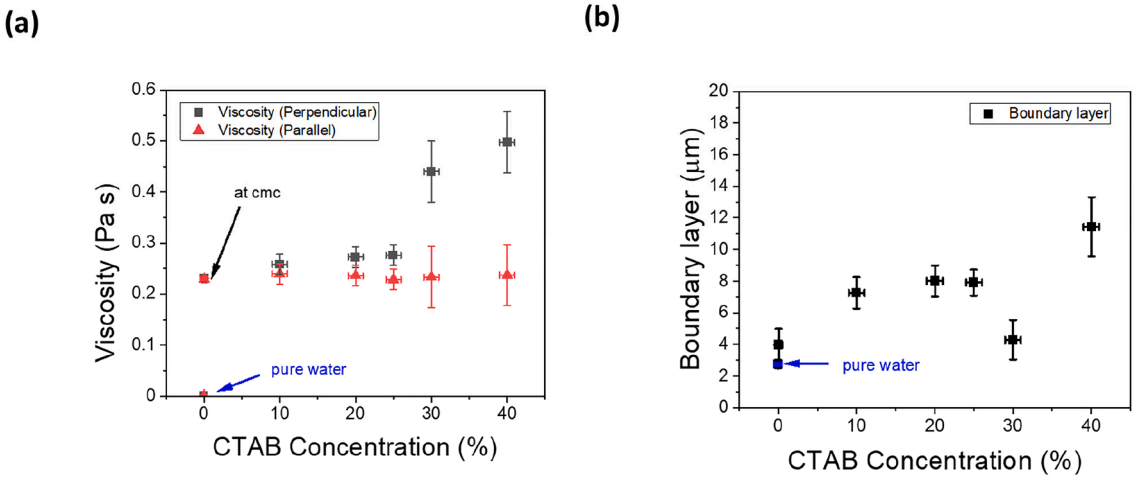

Fig. 6. (a) Concentration dependence of the viscosity of CTAB in the hexagonal phase. Already at very low concentrations above the cmc the viscosity is much larger than that of the solvent (water). (b) The boundary layer roughly increases for increasing CTAB concentration, while the value at very small concentration above the cmc is comparable to that of water.

hexagonal phase in the CTAB/water mixture. This is expected as with increase in viscosity, the boundary layer thickness should increase [27]. The uncertainty in the orientation is reflected in the large error bars in Fig. 6 (a).

4.5. Lyotropic chromonic Sunset Yellow (SSY)

The food coloring dye Sunset Yellow (SSY) is one of the standard chromonic LCs that forms chromonic stacks (Fig. 7) and lyotropic LC phases in aqueous solutions [28–30]. The concentration dependent viscosities and boundary layer thickness of the lyotropic nematic phase of aqueous SSY solutions were measured at room temperature using the oil-based ferrofluid EFH1. A comparison to the values obtained for the isotropic phase just above the cmc is made.

According to Israelachvili [31], the cmc is determined by $cmc \approx exp(-\alpha)$ where α is the average interaction energy (in units of k_BT). The value of α has been reported to be 7.25 by Horowitz et al., [32] and 11.10 ± 0.18 by Renshaw et al. [33]. This gives a relatively large concentration range for the cmc of 0.04–1.58 wt%. Fig. 8(a) depicts the concentration dependence of the viscosity. The viscosity is isotropic in the regime just around the cmc with a value $\gamma = 403 \pm 41$ mPa s at a concentration of 0.09 wt%. This value is significantly larger than that of deionized water by a factor of 400 and also an order of magnitude larger than that of a thermotropic nematic liquid crystal. In the chromonic nematic phase, which starts at a concentration of about 15 wt%, the viscosity is anisotropic and the difference between the perpendicular and parallel viscosity values with respect to the director, increases with increasing in concentration.

Interestingly, the boundary layer dependence on concentration (Fig. 8(b)) behaves quite differently from the previously observed behaviour for lyotropic CTAB. In the isotropic phase above the cmc, the boundary layer thickness is approximately ten times larger than that observed for a viscous isotropic fluid, which indicates that stacks are already formed, while being isotropically distributed in the water. For concentrations above the formation of the nematic phase, the boundary layer thickness decreases with increasing concentration. This might be caused by the plate-like structure of the molecules which may be easier to deform than the micellar structures of the amphiphilic lyotropic liquid crystals, in the same sense as the lamellar phase is less viscous than the hexagonal one.

4.6. Colloidal graphene oxide (GO)

GO is the oxygenated form of a monolayer graphene platelet with strong mechanical properties, chemical functionalization capability, and extremely large surface area [35]. GO readily forms lyotropic nematic phases in water and the director field orientation depends on the geometry of the cell [8,34–37].

For the closed sandwich cell, the same procedure which was used for the other LCs was utilized. For the closed cell measurements, the measured viscosity in the center is isotropic due to the director field aligning in the z-direction and the measurements can only be taken in the x-y plane (Fig. 9(a)). All viscosity measurements were taken in the central portion of each cell. To measure the anisotropic viscosities of the lyotropic nematic phase of aqueous solutions of GO, an uncoated open glass channel cell, similar to one used by Al-Zangana et al., [35] was employed in addition to the closed sandwich cell. For the open channel, two glass coverslips were placed on a glass microscope slide and fixated using UV glue, while producing a channel of millimeter width. This causes the GO molecules to align parallel to the cover slip edges as schematically shown in Fig. 9(b). The LC ferrofluid emulsion was deposited in this channel and measurements were taken parallel and perpendicular to the director, which can be defined as the cell normal. Both cell types are uncoated because the GO flakes strongly lie flat on the glass walls. The measurements were obtained using ferrofluid EFH1.

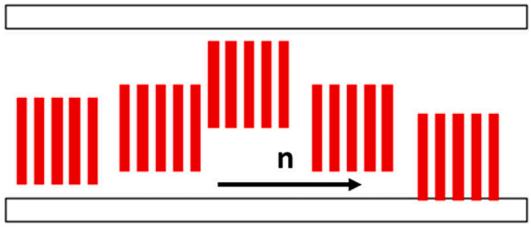

Fig. 7. Sideview of the structure of the low concentration lyotropic nematic phase of SSY. The SSY molecules form columnar stacks which act as cylinders and orient along a director. The low concentration phase of the chromonic Sunset Yellow is the nematic phase. (For interpretation of the references to colour in this figure legend, the reader is referred to the web version of this article.)

The concentration dependence of the viscosity for the closed cell, i.e., the isotropic viscosity perpendicular to the director, is depicted in Fig. 10(a). This viscosity exhibits a sudden increase during the transition from the isotropic to the nematic phase which occurs in approximately the concentration range of 0.75 − 1 wt% GO in water. After this transition, when the nematic phase is developed, the viscosity remains practically constant with change in concentration. The viscosity value observed in the isotropic phase of GO/water is clearly larger than that of the solvent by about two orders of magnitude, and comparable to that of micellar solutions just above the cmc. Similar to the chromonic plate-like dye molecules of sunset yellow, the thickness of the boundary layer decreases for GO in water with increasing concentration as shown in Fig. 10(b).

For the open cell, the determined viscosities are anisotropic, measured parallel and perpendicular to the director which is defined as the average GO plate normal. The relation between parallel and perpendicular viscosity with concentration is shown in Fig. 11(a). The perpendicular viscosity exhibits a sudden increase during the transition range from the isotropic to the nematic phase while the increase for the parallel viscosity is much less dominant. Within the nematic phase range, the two viscosities are constant within limits of error. The boundary layer thickness (Fig. 11(b)) exhibits a large variation without any clear trend. Given the variation, the errors are most likely underestimated so that no conclusions may be drawn about any concentration dependence. Yet, it is evident that the boundary layer thickness is of the same order of magnitude as that of lyotropic sunset yellow, and about a factor 5 larger than that of a standard thermotropic nematic (5CB).

4.7. Colloidal cellulose nanocrystals (CNC)

Cellulose nanocrystals (CNC) are H_2SO_4 treated cellulose crystallites which adopt a left-handed cholesteric (chiral nematic) liquid crystal phase [38] when dissolved in water. The concentration dependent viscosities of solutions of CNC and DI water were measured using the ferrofluid EFH1.

According to Honorato-Rios et al. [39], the CNC macroscopically phase separates in a sandwich cell into a two-phase system with some regions being mostly isotropic and others being largely cholesteric. For the below discussed measurements, we used ferrofluid droplets which were located in the cholesteric region of the cell. With increasing CNC concentration, the cholesteric region enlarged as expected and viscosity measurements were performed in the concentration range between 3 − 6 wt%. The cholesteric pitch is known to vary inversely with CNC concentration. It is thus expected that at higher concentrations, the pitch is approximately equal to the droplet diameter and so the measured viscosity is isotropic, as in the case for the thermotropic cholesteric (5CB + S811) discussed in Section 4.3.

As observed in Fig. 12(a), the difference between the parallel and the perpendicular viscosities of cellulose nanocrystals in water decreases with increasing concentration. This can be understood by the decreasing pitch of the cholesteric helical superstructure with increasing CNC

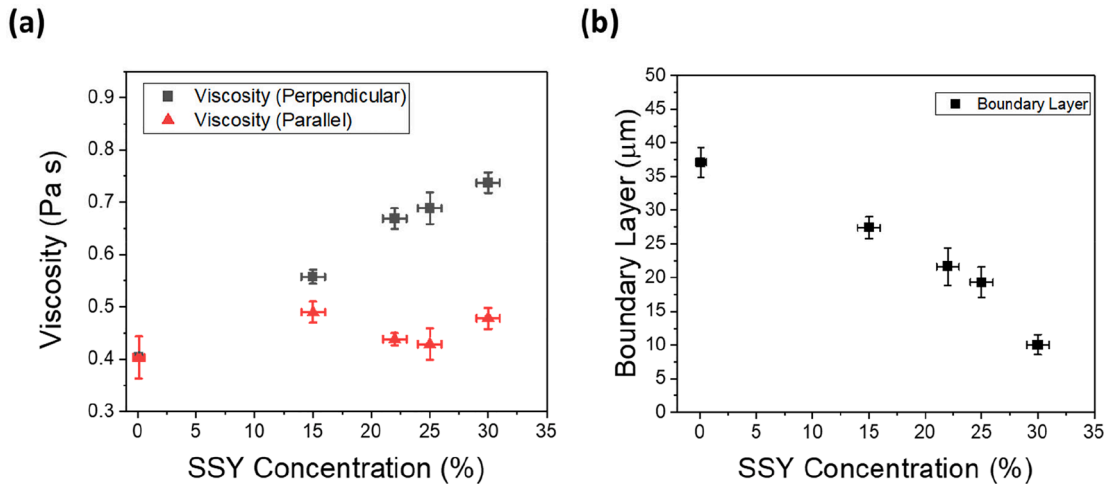

Fig. 8. (a) Concentration dependence of the viscosity of SSY. The chromonic nematic lyotropic liquid crystal phase is beginning to form at 15%. (b) Concentration dependence of the boundary layer thickness of Sunset Yellow.

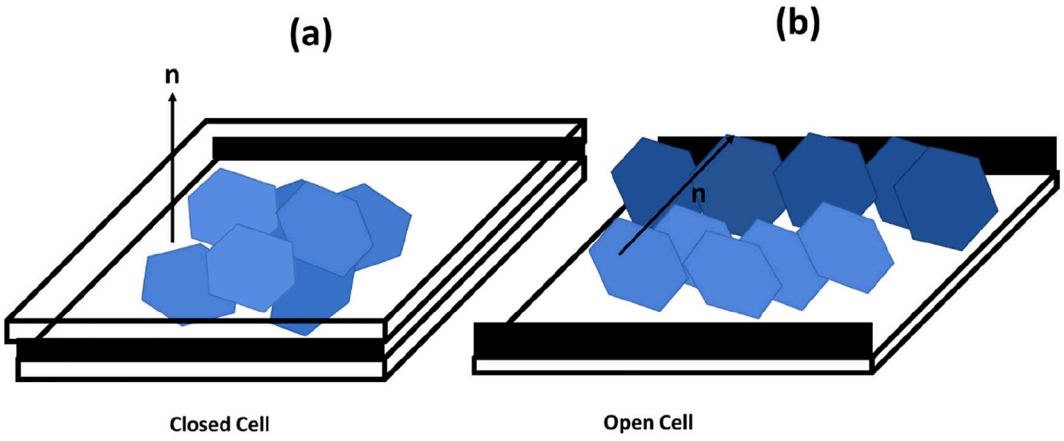

Fig. 9. Schematic illustration of the geometries of GO in (a) a closed cell and (b) an open channel.

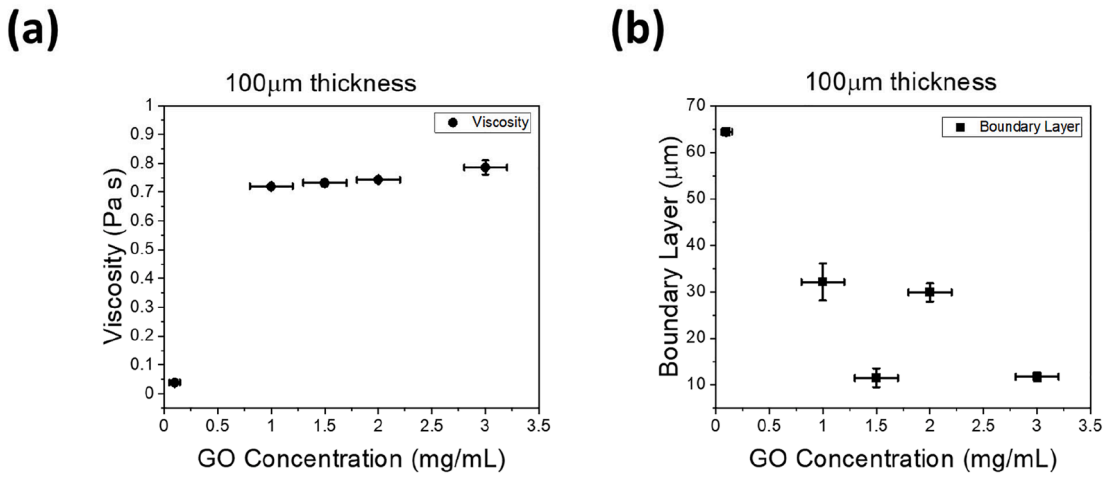

Fig. 10. (a) Concentration dependence of the viscosity of a GO/water lyotropic liquid crystal in a closed 100 μm thick cell. At very low concentrations, the system is isotropic while the transition to a nematic lyotropic phase occurs at concentrations of approximately 0.75–1 mg/mL. Given that measurements are taken perpendicular to the director, the viscosity is independent of direction in the plane of the cell. (b) Concentration dependence of the boundary layer thickness for a closed cell of GO/water.

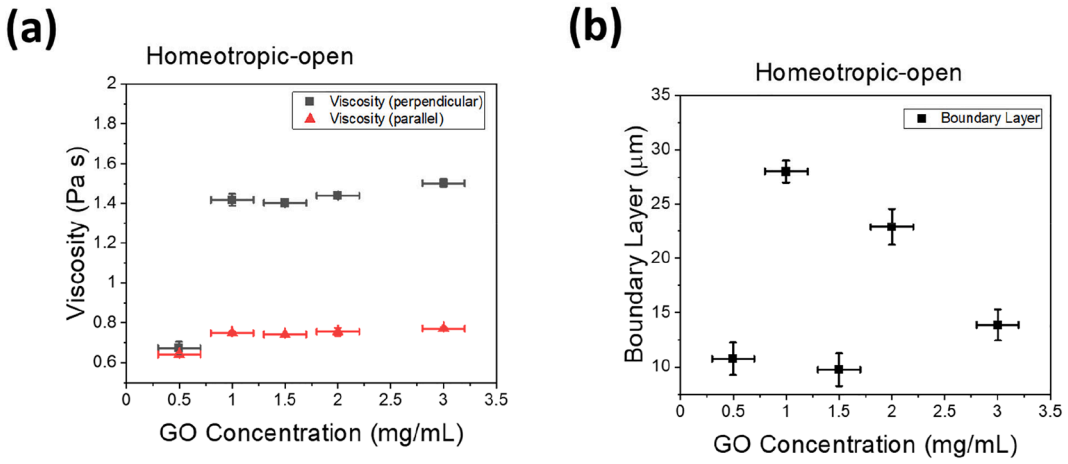

Fig. 11. (a) Concentration dependence of the viscosities of GO/water in the open channel geometry. (b) Concentration dependence of the boundary layer thickness.

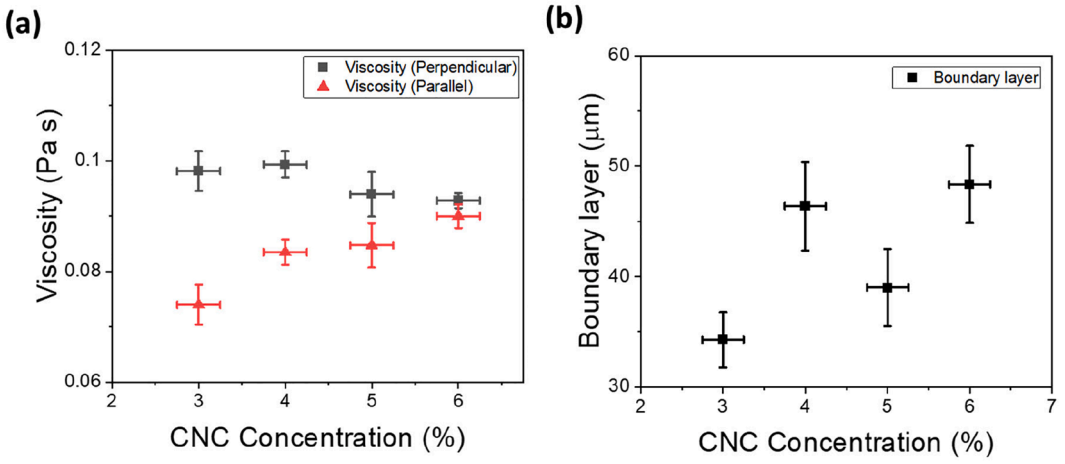

Fig. 12. (a) Concentration dependence of the viscosities for CNC/water. (b) Concentration dependence of the boundary layer thickness.

concentration as seen in Honorato-Rios et al. [39] and Mu et al., [40]. The behaviour is equivalent to that of the thermotropic case discussed in section 4.3 where the cholesteric pitch is decreased for increasing concentration of the chiral dopant. Here, the increasing CNC concentration decreases the pitch. While for low concentrations the cell boundary conditions deform the helical structure, a short pitch structure is accommodated within the cell without deformation. The ferrofluid droplet, depending on size of the cell, pitch and droplet diameter, can probe this deformation, which is reflected in the measured viscosities. This is equivalent to the above reported thermotropic cholesteric 5CB + S811 (in terms of concentration of S811), as expected. The boundary layer thickness values exhibit an increasing trend with increase in concentration (Fig. 12(b)) and the values are about an order of magnitude larger than those observed for a standard thermotropic chiral nematic liquid crystal. This is similar to the amphiphilic lyotropic LCs, and it can be concluded that the rod-like molecules exhibit the opposite trend to the plate like molecules observed for the lyotropic chromonic LCs and colloidal GO.

5. Conclusions

The viscosities of various types of LC phases; thermotropic, lyotropic, chromonic and colloidal, were measured on a microscopic scale using dispersed ferrofluid droplet inclusions. The temperature dependent values for the anisotropic viscosities which are parallel and perpendicular to the director of a thermotropic nematic phase very well reproduce previous measurements with other methods. They are also very well reproducible, and the methods are thus suitable to carry out viscosity probing on a very small scale with minute amounts of substance. No discontinuities in viscosities nor boundary layer thickness were observed at the nematic to smectic A transition, which suggests that the smectic layer formation represents only a small change to the structure of the system, which is in line with the common understanding of the smectic A phase from x-ray diffraction as a sinusoidal density distribution. For the helical chiral nematic structure, no anisotropy in the viscosity was observed for small pitch helices. Only when the pitch became comparable to either the cell gap or the ferrofluid droplet diameter did this anisotropy arise due to a distortion of the helical structure. This suggests that ferrofluid droplets may also be used as probes for director field deformations, if the droplet diameter can suitably be adjusted, for example via microfluidics.

Lyotropic phases are in general much more viscous than their thermotropic counterparts. This was demonstrated for an amphiphilic lyotropic liquid crystal, even just above the cmc in the isotropic phase. Once the hexagonal phase was formed, the viscosity became anisotropic with an increasing anisotropy that rises with increasing concentration. A similar behaviour was observed for the lyotropic chromonic LC sunset yellow, where the droplet boundary layers also became substantially thicker than that observed for pure water or even a thermotropic LC. Colloidal lyotropic liquid crystals were investigated on the form of GO/

water and CNC/water systems. The graphene oxide system was studied in two different geometries and exhibited a substantial viscosity as well as anisotropy, yet without any significant concentration variation. The cellulose nanocrystal system exhibited a similar behaviour as the thermotropic chiral nematic system with the difference that the viscosity anisotropy vanished for increasing CNC concentration. This is due to the decreasing pitch of the helical structure with increasing CNC concentration, thus the vanishing of the director field distortions from the helical superstructure.

The method of using dispersed ferrofluid droplets in liquid crystals thus opens a wide range of liquid crystal classes, types and phases to be studied with respect to their viscosities. For controlled droplet sizes, it also offers the possibility to be developed into a probe for locally deformed director fields.

Declaration of Competing Interest

The authors declare that they have no known competing financial interests or personal relationships that could have appeared to influence the work reported in this paper.

Data availability

Data will be made available on request.

References

[1] P.G. De Gennes, J. Prost, The physics of liquid crystals, Oxford University Press, Oxford, 1993.
[2] P.J. Collings, J.W. Goodby, Introduction to liquid crystals: Chemistry and physics, 2nd ed., CRC Press, Boca Raton, 2019.
[3] I. Dierking, S. Yoshida, T. Kelly, W. Pitcher, Liquid crystal–ferrofluid emulsions, Soft Matter 16 (2020) 6021–6031.
[4] Q. Li, Nanoscience with liquid crystals, From Self-Organized Nanostructures to Applications. Springer, New York, 2014.
[5] P. van der Schoot, Molecular theory of nematic (and Other) liquid crystals: An introduction. springer, Nature (2022).
[6] G. Vertogen, W.H. De Jeu, Thermotropic liquid crystals, Fundamentals. Springer, Berlin, 1988.
[7] I. Dierking, A.M.F. Neto, New Trends in lyotropic liquid crystals, Crystals 10 (7) (2020) 604.
[8] A.M.F. Neto, S.R. Salinas, The Physics of Lyotropic Liquid Crystals: Phase Transitions and Structural Properties, Oxford University Press, Oxford, 2005.
[9] I. Dierking, S. Al-Zangana, Lyotropic liquid crystal phases from anisotropic nanomaterials, Nanomaterials 7 (2017) 305.
[10] S.S. Funari, M.C. Holmes, G.J. Tiddy, Intermediate lyotropic liquid crystal phases in the C16EO6/water system, The Journal of Physical Chemistry 98 (11) (1994) 3015–3023.
[11] H. Kneppe, F. Schneider, N.K Sharma, N.K., A comparative study of the viscosity coefficients of some nematic liquid crystals, Berichte der Bunsengesellschaft für physikalische Chemie 85, (1981): 784-789.
[12] H. Kneppe, F. Schneider, Determination of the viscosity coefficients of the liquid crystal MBBA, Molecular Crystals and Liquid Crystals 65 (1981) 23–37.
[13] A.G. Chmielewski, Viscosity coefficients of some nematic liquid crystals, Molecular Crystals and Liquid Crystals 132 (1986) 339–352.
[14] Q. Liu, T. Asavei, T. Lee, H. Rubinsztein-Dunlop, S. He, I.I. Smalyukh, Measurement of viscosity of lyotropic liquid crystals by means of rotating laser-trapped microparticles, Optics Express 19 (2011) 25134–25143.
[15] A. Ansón-Casaos, J.C. Ciria, O. Sanahuja-Parejo, S. Víctor-Román, J.M. González-Domínguez, E. García-Bordejé, A.M. Benito, W.K. Maser, The viscosity of dilute carbon nanotube (1D) and graphene oxide (2D) nanofluids, Physical Chemistry Chemical Physics 22 (2020) 11474–11484.
[16] P. Poulin, H. Stark, T.C. Lubensky, D.A. Weitz, Novel colloidal interactions in anisotropic fluids, Science 275 (5307) (1997) 1770–1773.
[17] P. Poulin, V. Cabuil, D.A. Weitz, Direct measurement of colloidal forces in an anisotropic solvent, Physical Review Letters 79 (1997) 4862.
[18] A.F. Neto, M.M.F. Saba, Determination of the minimum concentration of ferrofluid required to orient nematic liquid crystals, Physical Review A 34 (1986) 3483.
[19] V. Fréedericksz, A. Repiewa, Theoretisches und experimentelles zur frage nach der natur der anisotropen flüssigkeiten, Z. Physik 42 (1927) 532–546.
[20] J. Li, Y. Huang, X. Liu, Y. Lin, L. Bai, Q. Li, Effect of aggregates on the magnetization property of ferrofluids: A model of gaslike compression, Science and Technology of Advanced Materials 8 (2007) 448–454.
[21] O.D. Lavrentovich, Transport of particles in liquid crystals, Soft Matter 10 (9) (2014) 1264–1283.
[22] I. Dierking, Chiral liquid crystals: Structures, phases, effects, Symmetry 6 (2014) 444–472.
[23] M.T. Yatcilla, K.L. Herrington, L.L. Brasher, E.W. Kaler, S. Chiruvolu, J. A. Zasadzinski, Phase behavior of aqueous mixtures of cetyltrimethylammonium bromide (CTAB) and sodium octyl sulfate (SOS), The Journal of Physical Chemistry 100 (1996) 5874–5879.
[24] Y. Shao, M. Iliut, I. Dierking, A. Vijayaraghavan, Hybrid molecular/mineral lyotropic liquid crystal system of CTAB and graphene oxide in water, Carbon 173 (2021) 105–114.
[25] D. Lombardo, P. Calandra, L. Pasqua, S. Magazù, Self-assembly of organic nanomaterials and biomaterials: the bottom-up approach for functional nanostructures formation and advanced applications, Materials 13 (2020) 1048.
[26] I. Garcia-Mateos, M. Mercedes Velazquez, L.J. Rodriguez, Critical micelle concentration determination in binary mixtures of ionic surfactants by deconvolution of conductivity/concentration curves, Langmuir 6 (1990) 1078–1083.
[27] H. Schlichting, J. Kestin, 1961, Boundary-layer theory, McGraw-Hill, New York, 1961.
[28] A.P. Ormerod, J.W. Jones, H. Wheatcroft, A. Alfutimie, G.J. Tiddy, The influence of polar additives on chromonic mesophase formation of edicol sunset yellow, Liquid Crystals 42 (2015) 772–782.
[29] A. Masters, Chromonic liquid crystals: More questions than answers, Liquid Crystals Today 25 (2016) 30–37.
[30] H.S. Park, L. Tortora, R.M. Vasyuta, A.B. Golovin, E. Augustin, D. Finotello, O. D. Lavrentovich, Lyotropic chromonic liquid crystals: Effects of additives and optical applications, The Korean Information Display Society (2007) 307–310.
[31] J.N. Israelachvili, Intermolecular and surface forces, Academic Press. Burlington, MA, 2011.
[32] V.R. Horowitz, L.A. Janowitz, A.L. Modic, P.A. Heiney, P.J. Collings, Aggregation behavior and chromonic liquid crystal properties of an anionic monoazo dye, Physical Review E 72 (2005) 041710.
[33] M.P. Renshaw, I.J. Day, NMR characterization of the aggregation state of the azo dye sunset yellow in the isotropic phase, The Journal of Physical Chemistry B 114 (2010) 10032–10038.
[34] Z. Xu, C. Gao, Aqueous liquid crystals of graphene oxide, ACS nano 5 (2011) 2908–2915.
[35] S. Al-Zangana, M. Iliut, M. Turner, A. Vijayaraghavan, I. Dierking, Confinement effects on lyotropic nematic liquid crystal phases of graphene oxide dispersions, 2D Materials 4 (2017) 041004.
[36] R. Narayan, J.E. Kim, J.Y. Kim, K.E. Lee, S.O. Kim, Graphene oxide liquid crystals: discovery, evolution and applications, Advanced Materials 28 (2016) 3045–3068.
[37] A.P. Draude, I. Dierking, Lyotropic liquid crystals from colloidal suspensions of graphene oxide, Crystals 9 (2019) 455.
[38] J.P.F. Lagerwall, C. Schütz, M. Salajkova, J. Noh, J. Hyun Park, G. Scalia, L. Bergström, Cellulose nanocrystal-based materials: From liquid crystal self-assembly and glass formation to multifunctional thin films, NPG Asia Materials 6 (2014) e80–e.
[39] C. Honorato-Rios, A. Kuhnhold, J.R. Bruckner, R. Dannert, T. Schilling, J.P. F. Lagerwall, Equilibrium liquid crystal phase diagrams and detection of kinetic arrest in cellulose nanocrystal suspensions, Frontiers in Materials (2016) 21.
[40] X. Mu, D.G. Gray, Formation of chiral nematic films from cellulose nanocrystal suspensions is a two-stage process, Langmuir 30 (31) (2014) 9256–9260.